DOI: 10.4149/BLL_2014_133

Bratisl Lek Listy 2014; 115 (11)
685 – 691

EXPERIMENTAL STUDY

The inhibition effect of expressions of miR-221 and miR-222 on glioma and corresponding mechanism

Zhang Z[1], Cui BZ[1], Wu LH[2], Xu QL[1], Wang Z[2], Yang B[2]

Department of Neurosurgery, People's hospital of Zhengzhou, Henan province, People's Republic of China.
boyang201339@163.com

Abstract: *Purpose:* This study was designed to investigate the expressions of genes miR-221 and miR-222 in glioma cells and elucidate the mechanism of the inhibition of expressions of miR-221 and miR-222 in glioma.
Methods: After being cultured, in vitro cells of U251 malignant glioma were divided into five groups, namely, blank control group, nonsense sequence ODN transfection group, AS-miR-221-ODN transfection group, AS-miR-222-ODN transfection group, AS-miR-221 ODN and AS-miR-222 0DN co-transfection group.
Results: The growth of the cells in AS-miR-221/222 group was significantly inhibited after transfection of 24 hours. Moreover, this inhibition degree became more apparent with prolonged time. The cell percentage in AS-miR-221/222 transfection group was 57.2 % in G0/G1 phase, 35.1 % in S phase, and 38.2 % in G2/M phase. The cell percentage in S phase was decreased. Cell cycle arrest was found in G0/G1 phase. Animal experiments showed that the glioma volume of AS-miR-221/222 treatment group was significantly different to that of the control group ($p < 0.05$). Furthermore, this difference gradually increased with time. It reached the maximum at the end of the observation period. In the U251 glioma specimens in AS-miR-221/222 treatment group, local glioma tissue developed necrosis foci. In addition, the nuclear size, color, heteromorphism, and new vessel number of these glioma tissues were decreased.
Conclusion: There are a series of abnormal miRNA expressions in glioma. Among them, miR-221 and miR -222 are clustered miR s with elevated expressions. The over-expressions of miR-221 and miR-222 can be considered as new molecular tags for human glioma *(Tab. 5, Fig. 4, Ref. 30)*. Text in PDF *www.elis.sk.*
Key words: miR-221, miR-222, glioma, inhibition, target gene.

Glioma is one of the most common primary intracranial tumors. It accounts for about 46 % of intracranial tumors. The incidence of malignant glioma is 5 ~ 8/100 000. According to the ranking of World Health Organization published in 1998 by mortality, malignant glioma ranks second for the tumor patients under 34 years old and fourth for the tumor patients 35 ~ 54 years old (1). Due to its invasive growth glioma cannot be completely cut off through surgery. Moreover, glioma cells can't be highly specifically destroyed by chemotherapy or radiotherapy. Thus treatment effect is poor. Meanwhile, toxic and side effects may be generated on central nervous system (2–3). The situation above has not been fundamentally improved in clinical practice in the past 30 years. Therefore, glioma is still a refractory disease in the neurosurgery field. Elucidating the pathogenesis of glioma and looking for new treatment methods are still hot topics in the neurosurgery field.

Current molecular pathology suggests that glioma is a polygene disorder disease in nature. The development process of glioma is indicated as: the over-expressions of one or more cancer genes plus the mutation and deletion of tumor suppressor genes induce the abnormality of signal transduction pathway. Thus glioma cells escape the normal growth regulation mechanism. By independent proliferation and invasion, they finally generate a malignant phenotype (4–5). Micro RNA (microRNA or miRNA) is a small non-coding RNA with a length of about 21 ~ 25 nucleotides. The studies in recent years found that miRNA could combine with the 3' noncoding region of target mRNA. Then through promoting the degradation of target mRNA and suppressing the translation of target mRNA at post-transcriptional level, miRNA could negatively regulate gene expression (6–7). Existing studies proved that more than 50 % of miRs were positioned in cancer related gene region or vulnerable region. Especially, it was found that the expressions of some miRs were completely different with those of tumor cells and normal cells. These results made people believe that miRs were related with tumor formation (8).

By investigating the miRs expression profiles of glioma, it was observed that the expressions of some miRs were different from those of normal astrocytes. In these miRs, the expressions of miR-221 and miR-222 were significantly higher than those of normal astrocytes (9). Therefore, some important issues are worth attention, i.e. what kind of target gene expression is regulated by miR-221 and miR-222 in promoting glioma formation? Whether or not the malignant phenotype of glioma can be reversed by knocking down the expressions of miR-221 and miR-222 and generate new therapeutic target for glioma? To solve these issues, this study focused on investigating the effect of miR-221 and miR-222 in the

[1]Department of Neurosurgery, People's hospital of Zhengzhou, Henan province, People's Republic of China, and [2]People's hospital of Zhengzhou, Henan province, People's Republic of China

Address for correspondence: Bo Yang, Department of Neurosurgery, The First Affiliated Hospital of Zhengzhou University, No. 1, Jianshe Road, Zhengzhou, Henan province, P.R. China, Zip code: 450052

malignant phenotype of glioma. Moreover, it confirmed the inhibitory effect of the reduction of miR-221 and miR-222 expressions on glioma growth through in vitro and in vivo studies.

Materials and methods

Materials

A total of 55 BALB/c-nu (SPF) female nude mice were used in this study. They were 6 ~ 8 weeks old and weighed18 ~ 20 g. These mice were purchased from Shanghai Slaccas Experimental Animal Limited Liability Company, China. The certificate number was SCXK (Shanghai) 2013-0003. Rearing conditions: the mice were raised in specific pathogen free (SPF) aseptic laminar flow room at constant temperature (22 °C ~ 25 °C) and constant humidity (55 ± 5 %) and fed with sterilized food and water.

U251 malignant glioma in vitro cells were purchased from Shanghai Yanjing Biological Research Technology Co. Ltd; miR-221/222 in-situ hybridization kit was purchased from Shanghai Weijing Biological Technology Co. Ltd; Diethylpyrocarbonate (DEPC) was purchased from American Fermentas Company; diamidino phenylindole (DAPI) nucleus assay kit was purchased from Beijing Biocoen Biotechnology Co. Ltd, China; TUNNEL in-situ apoptosis detection kit was purchased from American Santa-Cruz Company.

Culturing and grouping of glioma cells

U251 malignant glioma in vitro cells were digested using proper amount of 0.25 % trypsin. When the cells turned ground and had not floated up, a proper amount of complete culture liquid was added in. The cells obtained were blown repeatedly. Then frozen stock solution bearing 10 % glycerol was added in. After gradually cooling, the cells were reserved in liquid nitrogen. Then cells were resuscitated by rapid thawing in 37 °C water bath and then by adding complete culture liquid in appropriate amount. Eight hours after, complete culture liquid was replaced, and cells were normally sub-cultured. The obtained cells were divided into five groups in total, namely, blank control group (contro1), nonsense sequence ODN transfection group (scramble), AS-miR-221-ODN tranfection group(AS-miR-221), AS-miR-222-ODN transfection group (AS-miR-222), AS-miR-221 ODN and AS-miR-222 0DN co-transfection group (AS-miR-221/222).

Glioma cell proliferation activity analysis by MTT (methyl thiazolyl tetrazolium) colorimetric method

U251 cells were normally digested in their logarithmic growth phase. Then they were inoculated into 96 well plate, with 5000 (200 μL) for each well. Twenty-four hours later, they were conventionally transfected with scramble, AS-miR-221 ODN and AS-miR-222 ODN. After transfection, they were inspected using MTT on the 1st, 2nd, 3rd, 4th, and 5th day, respectively. MTT detection process was indicated as: MTT in concentration of 5 mg/ml was added in to the 96 well plate mentioned above by 20 μl for each well. After the cells were cultured at 37 °C for 4 hours, supernatant was discarded. Then each well was added with 200 μL DMSO and oscillated for 15 min. Finally, the absorbance of each well (A) was measured using the 570 nm wavelength of ultraviolet spectrophotometer. The mean values of each of the 8 wells were obtained. Glioma cell proliferation rate calculation method: glioma cell proliferation rate of test group was calculated using the glioma cells untransfected by ODN as a control.

Glioma cell cycle analysis by flow cytometry

Forty-eight hours after transfection, the U251 cells were fully digested into single cell suspension using appropriate amount of trypsin (0.125 %). The single cell suspension obtained was completely suspended using phosphate buffer solution (PBS) (0.01 M, pH .2) by centrifuging at 000 rpm×5 min and 4 °C. Next, they were centrifuged at 1000 rpm × 5 min and 4 °C twice. The cell suspension obtained was filtered using strainer of 400 mesh. After centrifugation, the cells were fixed for 24 h using 1 ml ethanol at a concentration of 75 % at 4 °C. Then ethanol was removed by centrifugation at 1000 rpm for 5 min at 4 °C. The cells obtained were washed twice by PBS (0.01 M, pH 7.2) at 4 °C. Then they were incubated at 37 °C for 30 min using 200 μL Ranse A (1mg/m1). After mixed with 800 μL PI staining solution, they were stained at 4 °C for 30 min by avoiding light. Finally, their cycle phase distribution was determined using flow cytometry. The percentage of DNA index and cells in each phase were calculated.

Glioma cell in vitro invasion test (Transwell test)

The U251 cells growing in well were the next day after subculture gently rinsed twice using serum-free DMEM medium. After serum-free medium was added these cells were cultured in incubator with 5 % CO_2 at 37 °C for 24 ~ 48 h. Then the cell culture supernatants were collected and centrifuged at 1200 rpm and 4 °C for 10 min. Supernatants were collected. Then they were filtered and sterilized using 0.22 μm filtering membrane. Finally, they were packed and preserved at 20 °C for utilization.

One hundred μL diluted Matrigel (3.9 μg/ μL) were added onto the polycarbonate membrane of Transwell upper chamber (6.5 mm in diameter). After placed at 37 °C for 30 min, they were polymerized into gel. Then 500 ml chemokine were added in Transwell lower chamber. The pretested cell serum-free mediums were processed into single cell suspensions, with three holes for each kind of cell. Then in to each upper chamber hole with $l \times 10^5$ cells and 100 ml cell suspension was added accurately. Then the upper chamber was placed in 5 % CO_2 incubator at 37 °C for cell culturing for 24 h. After culturing, the liquid in upper chamber was discarded and the upper chamber was carefully removed out. The cells did not pass through the membrane were wiped off using wet cotton swabs. The remaining cells were stained using hematoxylin. After being rinsed, they were bilaterally mounted by Clearmont and dried at 80 °C. The cells passing through membrane were directly observed under inverted microscope (200×). Then we randomly selected 5 visions from the central part or surrounding part of each membrane and counted the cells passing through 8 μ m micro-hole. U251 group, nonsense control group, and AS-miR-221/222 group were set, with 3 holes for each group.

Glioma cell suspension inoculation and experimental animal grouping

The U251 glioblastoma cells in logarithmic growth phase were digested using 0.125 % trypsin. They were then centrifuged at room temperature by1000 rpm × 10 min. After the supernatant removal, they were centrifugally washed twice using PBS. The cell number was counted. Then cell concentration was adjusted to 5×10^7/ml. The cells were made into cell suspension by being suspended in serum-free DMEM medium. Next, we extracted 200 µl of cell suspension using the syringe with No. 6 needle. The cell suspension was inoculated into the skin of axillas and groins of 5 nude mice. The 5 nude mice were taken as the first generation of glioma-bearing nude mice. The gliomas of these mice were then used as xenograft to the nude mice in other experiments.

The gliomas successfully transplanted by cell inoculation (about 5 mm in diameter) were grafted to the nude mice in other experiments. The process was indicated as: glioma-bearing nude mice were executed by hauling necks. Under sterile conditions, glioma tissues in appropriate size were cut from these mice and then immediately placed in serum-free DMEM medium. Then they were sheared. After fat and necrotic glioma tissues were removed, the remaining glioma tissues were washed with serum-free DMEM and cut into tumor tissue blocks in size of l mm^3 for inoculation. Before inoculation, the skin on the inoculation site was disinfected using iodine tincture and 75 % alcohol. Then a small incision was sheared on the left groin skin of each nude mouse using disinfected scissors. Subsequently, a small block was inoculcated under the skin along the incision using sterile forceps. Finally, the incision was disinfected using 75 % alcohol (10).

The gliomas of glioma-bearing nude mice in the first generation developed into gliomas with rapid and stable growth rate in nude mice after xenografting. Experimental groups: all index detections in this experiment were in accordance with the following groups: blank control group (contro1), nonsense sequences ODN transfection group (scramble), AS-miR-221-ODN transfection group (AS-miR-221), AS-miR-222-ODN transfection group (AS-miR-222), AS-miR-221 ODN and AS-miR-222 0DN co-transfection group (AS-miR-221/222), ten mice for each group.

Glioma growth observation

After glioma tissue blocks were inoculated into nude mice for about two weeks, subcutaneous glioma volume grew to about 50 mm^3, the glioma grew to about 5 mm in diameter. At this time, ODN mixture was injected by in-situ multiple points, treatment experiment of glioma followed. From the beginning of the first treatment, we performed one treatment every three days, and five treatments in total. Control group: each mouse was injected with 40 µl DMEM medium in each treatment; treatment group: each mouse was injected with 40 µl Lipofectamine 2000/ODN complexes in each treatment. From the beginning of the first treatment, the block lengths (a) and widths (b) of tissue blocks were measured using vernier caliper every 2 days. Glioma volumes were calculated by formula.

Conventional HE staining of glioma tissue specimens

After fixed, glioma tissue blocks were conventionally embedded in paraffin and then sliced into sections of 5 µm. Then the glioma tissue sections were de-waxed using xylene and hydrated using various levels of ethanol. Afterwards, they were stained by hematoxylin for 5min and washed by tap water. Subsequently, they were differentiated using hydrochloric acid alcohol for 30 s. Then they were immersed in water for 15 min and eosin for 5 min. Finally, they were dehydrated, clarified, mounted and observed using optical microscope.

Cell apoptosis of each glioma tissue group detected by TUNEL in-situ apoptosis kit

Paraffin sections were conventionally de-waxed to water. Then they were placed in 3 % H_2O_2 methanol for 30 min at room temperature to inactivate endogenous peroxidase. Subsequently, they were washed using 0.01 M PBS (pH 7.2) for 5 min three times. Glide covers were immersed using membrane liquid at room temperature for 30 minutes. Then they were added with 20 µl marking liquid and placed at 4 °C overnight. DAPI was diluted by 1 : 500 0.01 M PBS (pH 7.2) and used to re-dye the nucleus for 5 min. The obtained nuclei were washed using 0.01M PBS (pH 7.2) for 5 min, 3 times. After mounted, they were observed and pictured using laser confocal microscope.

Statistical analysis

The experimental data were statistically analyzed using SPSS 13 statistical software, X^2 test, and single factor variance analysis method, with $p < 0.05$ as test level.

Results

Cell proliferation rate analysis by MTT colorimetric method

Uncontrolled cell proliferation is the main malignant phenotype of glioma. In this study, we conducted dynamic observation of the proliferation of the U251 cells in each group using MTT method. The results showed that at the 24th, 48th, 72th, 96th, 120th hour after transfection, the cell growth in scramble

Tab. 1. Results of cell proliferation rate by MTT method.

Time	Control group	Scramble transfection group	AS-miR-221 group	AS-miR-222 group	AS-miR-221/222 group
24h	100±3.62	100±3.73	100±3.48	100±3.56	100±3.28
48h	100±3.68	90.38±3.82	89.35±3.52	85.16±3.48	73.62±3.67*
72h	100±3.72	93.67±3.65	75.36±3.71	72.61±3.87	54.87±3.71*
96h	100±3.81	95.71±3.92	58.39±3.67	56.12±3.69	33.19±3.85*
120h	100±3.90	92.32±3.99	64.58±3.96	62.91±3.83	34.75±3.42*

Comparing with control group, scramble tranfection group, AS-miR-221 tranfection group, AS-miR-222 transfection group, * $p < 0.05$.

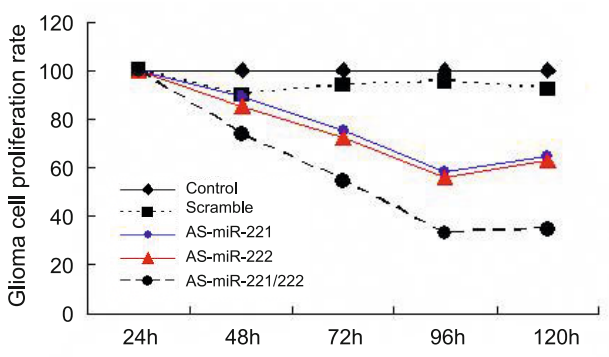

Fig. 1. MTT experiments showed that glioma cell proliferation decreased in AS-miR-221/222 treatment group.

transfection group was not inhibited significantly, while that of AS-miR-221/222 group was obviously inhibited at 24th hour after transfection. Moreover, with time the inhibition was more apparent. The cell growth of AS-miR-221 transfection group and AS-miR-222 transfection group were lower than that of the control group and the nonsense sequence transfection group. The cell growth of AS-miR-221/222 co-transfection group was much lower, as shown in Table 1 and Figure 1.

Cell cycle analysis by flow cytometry

Cell cycle is an important index to judge the state of cell proliferation. Cell cycle is generally divided into G0/G1 phase, S phase and G2/M phase, which correspond to earlier DNA synthesis stage, , later DNA synthesis stage, respectively. The cell percentage in S phase reflects the proliferation state of cell. The smaller the glioma cell percentage in S phase, the more effective the treatment. According to cell cycle analysis by flow cytometry, the U251 cell percentages of AS-miR-221 group, AS-miR-222 group, control group and nonsense sequence transfection group were 41.6 %, 38.4 %, 37.6 %, and 35.3 % in G0/G1 phase respectively; they were 63.1 %, 60.2 %, 65.2 % and 67.6 % in S phase; they were 25.3 %, 30.4 %, 24.8 % and 27.2 % in G2/M phase; the cell percentage of AS-miR-221/222 co-transfection group was 57.2 % in G0/G1 phase, 35.1 % in S phase, and 38.2 % in G2/M phase. These data suggested thatin AS-miR-221/222 co-transfection group, cell percentage in S phase was decreased and cell cycle arrest occurred in G0/G1 phase ($p = 0.007$). Moreover, compared with nonsense sequence transfection group and control group, AS-miR-221 group and AS-miR-222 group did not show significant G0/G1 phase arrest, as shown in Table 2.

Cell in vitro invasion test results (transwell test)

The cells that did not pass through the membrane were wiped out using wet cotton swabs. The remaining cells were stained using hematoxylin. We randomly selected 5 visions (100×) from the central and surrounding part of the counting membrane and counted the cell number in these visions. It was found that the mean numbers of invasion cells in the control group and blank loading group were 57.18 ± 2.67 and 59.36 ± 2.71, respectively; the mean number of invasion cells in AS-miR-221 group and AS-miR-222 group were 44.62 ± 2.41 and 41.84 ± 2.38; the mean number of invasion cells in AS-miR-221/222 co-transfection group were22.13 ±1.82, as shown in Table 3 and Figure 2.

Tab. 2. Cell cycle analysis results (%).

Group	G0/G phase	S phase	G2/M phase
Control group	37.6	65.2	24.8
Scramble transfection group	35.3	67.6	27.2
AS-miR-221 group	41.6	63.1	25.3
AS-miR-222 group	38.4	60.2	30.4
AS-miR-221/222 group	57.2*	35.1*	38.2*

Comparing with control group, scramble tranfection group, AS-miR-221 tranfection group, AS-miR-222 transfection group, * $p < 0.05$.

Tab. 3. The invasion of U251 cell strain measured by transwell in vitro invasion test.

Group	The cells passing through membrane
Control group	57.18±2.67
Scramble transfection group	59.36±2.71
AS-miR-221 group	44.62±2.41
AS-miR-222 group	41.84±2.38
AS-miR-221/222 group	22.13±1.82*

Comparing with control group, scramble tranfection group, AS-miR-221 tranfection group, AS-miR-222 transfection group, * $p < 0.05$.

Nude mice subcutaneously inoculated with glioma blocks

The glioma blocks subcutaneously inoculated to 55 nude mice all developed into gliomas a week later, with formation rate of 100 %. Glioma size was 48.72 +3 .76 mm^3. Except for 5 tumor-bearing nude mice of the first generation, the remaining 50 nude mice all received glioma xenograft. Then they were randomly divided into 5 groups, with 10 mice for each group.

Glioma growth inhibition state

The cell growth in U251 glioma AS-miR-221/222 treatment group was slower than that in control group. Moreover, 4 days after inoculation, the growth rate was not significantly accelerated. According to the measurement results before the 4th day, although the glioma growth rate of AS-miR-221/222 group was relatively lower, the difference did not have statistical significance comparing with control group and nonsense sequence transfection group ($p > 0.05$). From the 6th day, the glioma volume in AS-miR-221/222

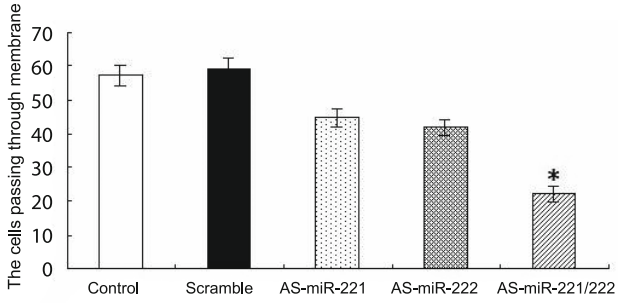

Fig. 2. The invasion of U251 cell strain measured by transwell in vitro invasion test. Comparing with control group, scramble tranfection group, AS-miR-221 tranfection group, AS-miR-222 transfection group, * $p < 0.05$.

Tab. 4. The growth inhibition condition of U251 glioma after being transplanted into nude mice.

Time	Control group	Scramble transfection group	AS-miR-221 group	AS-miR-222 group	AS-miR-221/222 group
0d	49.2±2.3	48.3±2.4	48.7±2.2	47.6±2.5	47.9±2.3
3d	51.3±2.4	52.7±2.8	50.3±2.4	49.2±2.3	48.1±2.2
6d	73.7±2.5	78.4±2.6	67.2±2.5	65.6±2.2	52.2±2.5*
9d	84.2±2.9	89.6±2.9	74.2±2.6	71.1±2.6	58.6±2.4*
12d	98.6±3.3	101.7±3.0	88.7±2.9	82.2±3.0	63.5±2.7*
15d	112.3±3.7	119.2±3.5	94.3±2.8	90.1±3.1	69.1±2.9*

Comparing with control group, scramble tranfection group, AS-miR-221 tranfection group, AS-miR-222 transfection group, * $p < 0.05$.

Tab. 5. Glioma tissue apoptosis detected by TUNEL method.

Group	Apoptosis index
Control group	3.95±0.42
Scramble transfection group	4.41±0.53
AS-miR-221 group	8.96±1.62
AS-miR-222 group	10.17±2.04
AS-miR-221/222 group	21.64±3.91*

Comparing with control group, scramble tranfection group, AS-miR-221 tranfection group, AS-miR-222 transfection group, * $p < 0.05$.

group was significantly different to that in the control group ($p < 0.05$). Moreover, with time , this difference gradually increased. To the end of the observation period, it reached the maximum. But there was no difference between nonsense sequence transfection group and control group ($p > 0.05$). Besides, the growth rates of AS-miR-221 group and AS-miR-222 group were lower than those of nonsense sequence transfection group and control group, but significantly faster than the AS-miR-221/222 treatment group, as shown in Table 4.

When gliomas were peeled after mice were killed, part of gliomas of the control group and nonsense sequence transfection group were observed with significant hemorrhage, liquefaction, and necrosis. These phenomena were in agreement with the growth characteristics of malignant glioma; while in AS-miR-221/222 treatment group, except individual gliomas, gliomas were all substantive. Moreover, obvious liquefaction was not found. Sporadic necrosis was observed on local glioma tissue occasionally. The performances of AS-miR-221 group and AS-miR-222 group were close to those of control group and nonsense sequence transfection group.

Glioma pathological changes detected by HE staining

We detected and analyzed the results obtained by performing HE staining of the tissue sections of glioma specimens. In the U251 glioma specimens in AS-miR-221/222 treatment group, local

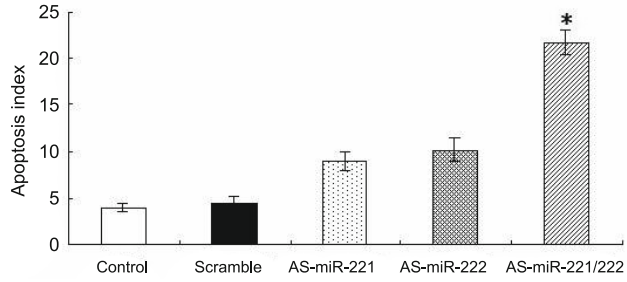

Fig. 4. U25l glioma cell apoptosis curve. Comparing with control group, scramble tranfection group, AS-miR-221 tranfection group, AS-miR-222 transfection group, * $p < 0.05$.

glioma tissue developed necrosis foci. The nuclear size, color, heteromorphism, and new vessel number of these glioma tissues were decreased. While in the control group and the nonsense sequence transfection group, glioma cells presented vigorous growth, large nuclear, deep color, and significant heteromorphism. Moreover, the new vessels in the two groups were more than that in AS-miR-221/222 treatment group, as shown in Figure 3.

Glioma tissue apoptosis detected by TUNEL method

Fluorescence microscopy observation displayed that the apoptosis index was 21.64 ± 3.91 in U25l in the glioblastoma subcutaneous glioma-bearing model AS-miR-221/222 treatment group. Compared with and that of control group (3.95 ± 0.42) and nonsense sequence transfection group (4.41 ± 0.53), there was statistically significant difference ($p < 0.05$). While in As-miR-221 treatment group, apoptosis index was 8.96 ± 1.62. In AS-miR-222 treatment group, the apoptosis index was 10.17 ± 2.04. The apoptosis indexes of As-miR-221 treatment group and As-miR-222 treatment group were higher than that of control group and nonsense sequence transfection group. But they were far lower than that of AS-miR-221/222 treatment group, as shown in Table 5 and Figure 4.

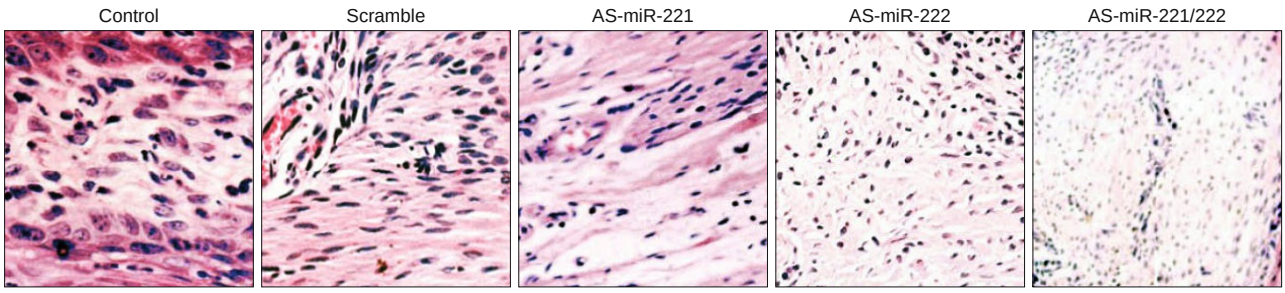

Fig. 3 Pathological changes of the transplanted glioblastoma of U251glioblastoma detected by HE staining.

Discussion

Cell cycle is divided into five phases, namely G0 phase (stationary phase), G1 phase, S phase, G2 phase and M phase. G1phase refers to the stage from mitosis completion to DNA replication. The activities in this phase mainly prepare for DNA replication and protein synthesis. S phase mainly includes the whole process of DNA replication and genetic material developing from diploid to tetraploid. G2 phase denotes the phase from DNA replication completion to mitosis beginning. In this phase, cells are observed with two sets of diploid chromosomes (11–12). Thus this phase is the mitosis phase. Cells begin to divide in M phase. At the end of M phase, two new sub-cells are formed. A cell cycle is ended. Then cell enters into the G1 phase of the next cell cycle, or stationary phase G0 (13). The analysis on cell cycle showed that after miR-221/222 expression are knocked down, AS-miR-221/222 effectively interferes with the mitosis of glioma celsl by blocking the glioma cells in G0/G1 phase.

At present, malignant glioma is mainly treated by combining intraoperative resection with postoperative radiotherapy and chemotherapy, etc. Due to the invasive growth of glioma, tumor boundaries are difficult to be determined. Besides, since some gliomas are located in main functional areas, the focus cannot be cut off completely during surgery (14). Meanwhile, because of the resistance of a majority of malignant glioma cells to radiotherapy and chemotherapy, the side effects of radiotherapy and chemotherapy, and the influences of blood brain barrier on chemotherapy drugs entering into glioma tissue, treatment effect is not ideal (15). In comparison, gene therapy method can treat glioma from pathogenesis (16). Since glioma is a polygene disease, previous single gene therapy presents poor effect by clinical validation (17). With further studies on miRNAs, single-target polygene therapy can possibly be performed.

Angiogenesis and tumor cell heteromorphism are important indexes in evaluating the malignant degree of the tumor (18). The more new vessels in the tumor tissue, the higher the blood supply obtained by tumor cells, and the more exuberant the tumor growth (19). Moreover, tumor cells can generate invasion and metastasis by destroying the basement membrane and entering into the blood circulation via vascular endothelium by many ways (20). After expressions of miR-221 and miR-222 are knocked down, the number of new vessels in tumor is reduced. Correspondingly, the nutrients obtained by tumor cells are decreased. This situation blocks the proliferation of tumor cells. Compared with in vitro experiments, the pathological changes of tumor can be more directly evaluated during in vivo experiments. Through the direct observation to the HE stained pathological sections, it is found that the new vessels in the malignant glioma treated by AS-miR-221/222 were significantly lower than those of control group and nonsense sequence transfection group; the heteromorphism of glioma cell was reversed to some extent; local glioma cell developed necrosis foci.

The heterogeneity expressed by the miRNAs in the glioma tissue of glioma patients provides very good molecular tags. By combining with tissue pathology detection, the biological behavior and response to treatment of glioma can be adequately predicted. Since the miRNAs expression of tumor is significantly different to that of surrounding normal tissues, tumor diagnosis is provided with basis (21–22). In fact, the specific expression profiles of tumor tissue are conductive to the discrimination on normal tissue and tumor tissue, such as in liver cancer, breast cancer, glioblastoma, papillary thyroid carcinoma, hepatocellular carcinoma, lung cancer, colon cancer and pancreatic cancer (23–24). Simultaneously, according to the specific miRNAs expression profiles of tumor tissue, the origin and development stages of tumor can be accurately judged. Moreover, the tissue origin of metastasis with unknown origin can be determined. Yang et al confirmed the miRNAs expression associated with tumor in the serous fluid of oral cancer patients was significantly higher than that of healthy people (25). Wurz et al found that the expression profiles of the exosome miRNAs released by tumor of ovarian cancer patients were highly similar with those of tumor miRNAs (exosome refers to the microbubbles containing RNAs and protein released by tumor cells or normal cells and formed in internal phagocytosis) (26).

Currently, a lot of evidences proved that tumor tissues showed miRNAs abnormal expression. The abnormal expressions are exhibited as the increased expression of tumor-promoter miRNAs in tumor or decreased expression of tumor-suppressor miRNAs in tumor (27). Thus miRNAs can be taken as a therapeutic target. By inhibiting the over-expressed miRNAs or promoting the low-expressed miRNAs, the miRNAs with abnormal expression can be corrected. By this way, the purpose of treating tumor can be achieved. At present, there are in vitro and in vivo researches investigating miRNAs activity inhitbition by artificially synthesizing antisense oligonucleotides that are mutually complemented with mature miRNAs or the precursor sequence of mature miRNAs (28). Meanwhile, to improve treatment options, antisense oligonucleotides are tested with various chemical modifications. These chemical modifications include the modification on the second hydroxyl of antisense oligonucleotides (adding methyl, methoxyethyl, fluorine radicals, or locked nucleotide), and the modification or phosphorothioate connection on thiophosphoric acid skeleton (29). With these modifications, the antisense oligonucleotides modified by locked nucleotide are more stable. They show strong affinity and low toxicity. Thus they begin to be used in clinical practice (30).

References

1. Xiao Y, Ping Y et al. Identifying dysfunctional miRNA-mRNA regulatory modules by inverse activation; cofunction; and high interconnection of target genes: A case study of glioblastoma. Neuro Oncol 2013; 17 (2): 135–137.

2. Tang W, Duan J et al. Subtyping glioblastoma by combining miRNA and mRNA expression data using compressed sensing–based approach. EURASIP J Bioinform Syst Biol 2013; 1 (2): 74–76.

3. Niyazi M, Zehentmayr F et al. MiRNA expression patterns predict survival in glioblastoma. Radiat Oncol 2011; 6: 153–155.

4. Galardi S, Mercatelli N et al. NF-kB and c-Jun induce the expression of the oncogenic miR-221 and miR-222 in prostate carcinoma and glioblastoma cells. Nucleic Acids Res 2011; 39 (9): 3892–3902.

5. Teixeira AL, Gomes M et al. EGFR signaling pathway and related-miRNAs in age-related diseases: the example of miR-221 and miR-222. Front Genet 2012; 3: 286–288.

6. Mardente S, Mari E et al. HMGB1 induces the overexpression of miR-222 and miR-221 and increases growth and motility in papillary thyroid cancer cells. Oncol Rep 2012; 28 (6): 2285–2289.

7. Yu B, Zhou S et al. miR-221 and miR-222 promote Schwann cell proliferation and migration by targeting LASS2 after sciatic nerve injury. J Cell Sci 2012; 125 (11): 2675–2683.

8. Amankwah EK, Anegbe E et al. miR-21; miR-221 and miR-222 expression and prostate cancer recurrence among obese and non–obese cases. Asian J Androl 2013; 15 (2): 226–230.

9. Wang X, Han L et al. Adenovirus-mediated shRNAs for co-repression of miR-221 and miR-222 expression and function in glioblastoma cells. Oncol Rep 2011; 25 (1): 97–105.

10. Keir ST, Friedman HS et al. Mibefradil a novel therapy for glioblastoma multiforme: cell cycle synchronization and interlaced therapy in a murine model. J Neurooncol 2013; 111 (2): 97–102.

11. Wu J, Fang J et al. Wnt inhibitory factoR-1 regulates glioblastoma cell cycle and proliferation. J Clin Neurosci 2012; 19 (10): 1428–1432.

12. Serao NV, Delfino KR et al. Cell cycle and aging; morphogenesis; and response to stimuli genes are individualized biomarkers of glioblastoma progression and survival. BMC Med Genomics 2011; 4: 49–53.

13. Alexander BM, Pinnell N et al. Targeting DNA repair and the cell cycle in glioblastoma. J Neurooncol 2012; 107 (3): 463–477.

14. Janardhanan R, Banik NL et al. N-(4-Hydroxyphenyl)retinamide induced differentiation with repression of telomerase and cell cycle to increase interferon–gamma sensitivity for apoptosis in human glioblastoma cells. Cancer Lett 2008; 261 (1): 26–36.

15. Liu H, Li Y et al. Clotrimazole induces a late G1 cell cycle arrest and sensitizes glioblastoma cells to radiation in vitro. Anticancer Drugs 2010; 21 (9): 841–849.

16. Lang MF, Yang S et al. Genome-wide profiling identified a set of miRNAs that are differentially expressed in glioblastoma stem cells and normal neural stem cells. PLoS One 2012; 7 (4): 248–251.

17. Nikaki A, Piperi C et al. Role of microRNAs in gliomagenesis: targeting miRNAs in glioblastoma multiforme therapy. Expert Opin Investig Drugs 2012; 21 (10): 1475–1488.

18. Visani M, Biase D et al. Definition of miRNAs expression profile in glioblastoma samples: the relevance of non-neoplastic brain reference. PLoS One 2013; 8 (1): 314–316.

19. Dong H, Luo L et al. Integrated analysis of mutations; miRNA and mRNA expression in glioblastoma. BMC Syst Biol 2010; 4: 163–165.

20. Roth P, Wischhusen J et al. A specific miRNA signature in the peripheral blood of glioblastoma patients. J Neurochem 2011; 118 (3): 449–457.

21. Kedde M, Kouwenhove M et al. A Pumilio-induced RNA structure switch in p27–3' UTR controls miR-221 and miR-222 accessibility. Nat Cell Biol 2010; 12 (10): 1014–1020.

22. Zhang CZ, Zhang JX et al. MiR-221 and miR-222 target PUMA to induce cell survival in glioblastoma. Mol Cancer 2010; 9: 229–233.

23. Karakatsanis A, Papaconstantinou I et al. Expression of microRNAs; miR-21; miR-31; miR-122; miR-145; miR-146a; miR-200c; miR-221; miR-222; and miR-223 in patients with hepatocellular carcinoma or intrahepatic cholangiocarcinoma and its prognostic significance. Mol Carcinog 2013; 52 (4): 297–303.

24. Shah MY, Calin GA et al. MicroRNAs miR-221 and miR-222: a new level of regulation in aggressive breast cancer. Genome Med 2011; 3 (8): 56–58.

25. Yang CJ, Shen WG et al. miR-221 and miR-222 expression increased the growth and tumorigenesis of oral carcinoma cells. J Oral Pathol Med 2011; 40 (7): 560–566.

26. Wurz K, Garcia RL et al. MiR-221 and MiR-222 alterations in sporadic ovarian carcinoma: Relationship to CDKN1B; CDKNIC and overall survival. Genes Chromosomes Cancer 2010; 49 (7): 577–584.

27. Koelz M, Lense J et al. Down-regulation of miR-221 and miR-222 correlates with pronounced Kit expression in gastrointestinal stromal tumors. Int J Oncol 2011; 38 (2): 503–511.

28. Loftus JC, Ross JT et al. miRNA expression profiling in migrating glioblastoma cells: regulation of cell migration and invasion by miR-23b via targeting of Pyk2. PLoS One 2012; 7 (6): 818–821.

29. Jethwa K, Wei J et al. miRNA-mediated immune regulation and immunotherapeutic potential in glioblastoma. Clin Investig (Lond) 2011; 1 (12): 1637–1650.

30. Sasaki A, Udaka Y et al. Analysis of p53 and miRNA expression after irradiation of glioblastoma cell lines. Anticancer Res 2012; 32 (11): 4709–4713.

Received May 10, 2013.
Accepted April 20, 2014.